Semiconductor quantum well irradiated by a two-mode electromagnetic field as a terahertz emitter

S. Mandal,[1] T. C. H. Liew,[1] and O. V. Kibis[2,1,*]

[1]*Division of Physics and Applied Physics, School of Physical and Mathematical Sciences, Nanyang Technological University, Singapore 637371, Singapore*

[2]*Department of Applied and Theoretical Physics, Novosibirsk State Technical University, Karl Marx Avenue 20, Novosibirsk 630073, Russia*

(Received 15 November 2017; published 26 April 2018)

We study theoretically the nonlinear optical properties of a semiconductor quantum well (QW) irradiated by a two-mode electromagnetic wave consisting of a strong resonant dressing field and a weak off-resonant driving field. In the considered strongly coupled electron-field system, the dressing field opens dynamic Stark gaps in the electron energy spectrum of the QW, whereas the driving field induces electron oscillations in the QW plane. Since the gapped electron spectrum restricts the amplitude of the oscillations, the emission of a frequency comb from the QW appears. Therefore, the doubly driven QW operates as a nonlinear optical element which can be used, particularly, for optically controlled generation of terahertz radiation.

DOI: 10.1103/PhysRevA.97.043860

I. INTRODUCTION

Recently, lasers and microwave techniques have been actively exploited to control the nonlinear optoelectronic properties of various systems with a strong high-frequency electromagnetic field (dressing field). Since the field is intense, the mixing of electron-field states results in a strongly coupled light-matter object known as an electron dressed by the field (dressed electron) [1,2]. The physical properties of dressed electrons can be described within the conventional Floquet theory of periodically driven quantum systems [3–6] and have been studied for various nanostructures, including semiconductor quantum wells [7–11], quantum dots [12,13], quantum rings [14–17], graphene [18–22], etc. Among a variety of nonlinear optical phenomena induced by a dressing field, the opening of dynamic Stark gaps in electron energy spectra of various condensed-matter structures should be noted especially (see, e.g., Refs. [8,14,23–25]). In the present paper, we demonstrate theoretically that this nonlinear effect results in the emission of a terahertz frequency comb from a semiconductor quantum well (QW) irradiated by a two-mode electromagnetic field.

II. MODEL

Let us consider a two-dimensional electron gas (2DEG) in a semiconductor QW irradiated by a linearly polarized two-mode electromagnetic wave, which propagates along the z axis and consists of a strong high-frequency dressing field, $\widetilde{E}\cos\omega_0 t$, with the electric-field amplitude $\widetilde{E}$ and the frequency ω_0, and a relatively weak and low-frequency driving field, $E\cos\omega t$, with the electric-field amplitude E and the frequency ω [see Fig. 1(a)]. In what follows, we will assume that the dressing field frequency ω_0 satisfies the condition $\hbar\omega_0 > \varepsilon_g$, where ε_g is the band gap of the QW. In this case, the dressing field strongly mixes electron states from the valence and conduction bands and, therefore, substantially modifies their energy spectrum due to the dynamic Stark effect. Particularly, the dressing field opens energy gaps, $\Delta\varepsilon$, within the bands in the resonant points of the Brillouin zone, k_0, where the photon energy $\hbar\omega_0$ is equal to the energy interval between the bands [23]. This gap opening is shown schematically in Figs. 1(b) and 1(c), where the first valence and conduction sub-bands of the QW are plotted in the Schrödinger and interaction pictures, correspondingly. For definiteness, we will restrict the following analysis by the Schrödinger picture. In the most general case, the energy spectrum of dressed electrons arising from any two bands mixed by the dressing field, $\varepsilon^+(\mathbf{k})$ and $\varepsilon^-(\mathbf{k})$, can be written in the form [8]

$$\varepsilon(\mathbf{k}) = \frac{\varepsilon^+(\mathbf{k}) + \varepsilon^-(\mathbf{k})}{2} \pm \frac{\hbar\omega_0}{2} \pm \frac{\alpha(\mathbf{k})}{2|\alpha(\mathbf{k})|}\sqrt{(\hbar\Omega_R)^2 + \alpha^2(\mathbf{k})}, \tag{1}$$

where $\alpha(\mathbf{k}) = \varepsilon^+(\mathbf{k}) - \varepsilon^-(\mathbf{k}) - \hbar\omega_0$ is the resonance detuning, $\mathbf{k}$ is the electron wave vector, $\Omega_R = d\widetilde{E}/\hbar$ is the Rabi frequency of interband electron transitions, and d is the interband dipole moment. In the considered case of a semiconductor QW, these two branches, $\varepsilon^+(\mathbf{k})$ and $\varepsilon^-(\mathbf{k})$, should be treated as the first electron sub-band, $\varepsilon^+(\mathbf{k}) = \hbar^2k^2/2m_e + \varepsilon_g/2$, and the first hole sub-band, $\varepsilon^-(\mathbf{k}) = -\hbar^2k^2/2m_h - \varepsilon_g/2$, where m_e and m_h are the electron and hole masses, respectively, and $\mathbf{k} = (k_x, k_y)$ is the electron wave vector in the QW plane. Since the dynamic Stark gaps, $\Delta\varepsilon = \hbar\Omega_R$, break the dispersion curves [Eq. (1)] only at the border wave vector, $|\mathbf{k}| = k_0$, the energy spectrum [Eq. (1)] around the ground state of the conduction band [see the red dot in Fig. 1(b)] is continuous and can be written as

$$\varepsilon_e(\mathbf{k}) = \frac{\hbar^2k^2}{2m_-} + \frac{\hbar\omega_0}{2} - \frac{1}{2}\sqrt{(\Delta\varepsilon)^2 + \left[\hbar\omega_0 - \varepsilon_g - \frac{\hbar^2k^2}{2m_+}\right]^2}, \tag{2}$$

where $m_\pm = m_e m_h/(m_e \pm m_h)$ is the reduced electron-hole mass, the electron wave vector $\mathbf{k}$ lies within the range $|\mathbf{k}| \leqslant k_0$,

*Oleg.Kibis@nstu.ru

 ©2018 American Physical Society

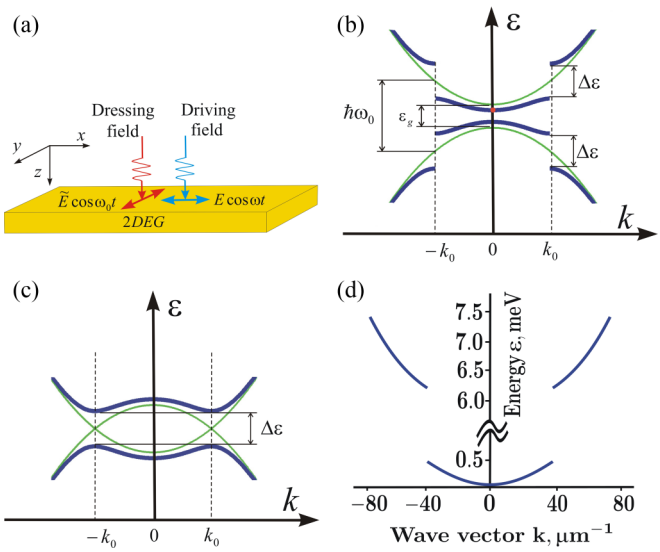

FIG. 1. Sketch of the system under consideration. (a) A 2DEG in a semiconductor QW irradiated by a two-mode electromagnetic field consisting of a dressing field, with the electric-field amplitude $\widetilde{E}$ and the frequency ω_0, and a driving field, with the electric-field amplitude E and the frequency ω. (b) Energy spectrum of the first conduction and valence sub-bands of the QW with the band gap ε_g, in the presence of the dressing field (the heavy blue lines) and without the field (the thin green lines) in the Schrödinger picture. Due to the gaps, $\Delta\varepsilon$, induced by the dressing field, the driving field can move a conduction electron (the red dot) along the dispersion curve only between the states $-k_0$ and k_0. (c) Energy spectrum of the first conduction and valence sub-bands of the QW in the presence of the dressing field (the heavy blue lines) and without the field (the thin green lines) plotted in the interaction picture. (d) Energy spectrum of the first electron sub-band in a GaAs-based QW irradiated by a dressing field with the frequency $\hbar\omega_0 = \varepsilon_g + 1$ meV and the amplitude $\widetilde{E} = 10^7$ V/m.

and the border wave vector k_0 satisfies the condition $\hbar\omega_0 = \varepsilon_g + \varepsilon_0$ with the characteristic border electron energy, $\varepsilon_0 = \hbar^2 k_0^2/2m_+$. It should be stressed that the dressing field amplitude, $\widetilde{E}$, is assumed to satisfy the strong light-matter coupling condition, $\Omega_R\tau \gg 1$, where τ is the mean free time of conduction electrons in the QW. In this regime, the interband absorption of the dressing field is absent (see, e.g., Ref. [8]) and, therefore, the dressing field does not generate electron-hole pairs. As to the driving field, its frequency is relatively low, $\hbar\omega \ll \varepsilon_g$. Therefore, the off-resonant driving field does not mix almost electronic states from the conduction and valence bands and, correspondingly, does not change the energy spectrum [Eq. (1)] renormalized by the resonant dressing field. Thus, the driving field results only in the electron transitions between different states of the continuous spectrum [Eq. (2)], which can be described within the conventional semiclassical approach as follows. First of all, it should be stressed that the magnetic component of the driving field lies in the plane (x,y). Since the electron velocities in the QW, $\mathbf{v} = (v_x, v_y)$, lie in the same plane, the Lorentz force caused by the magnetic field is directed perpendicularly to the QW. Therefore, it cannot affect electron dynamics in the QW plane. As a consequence, the dynamics of dressed electrons in the QW depends only on the electric component of the driving field, $\mathbf{E} = (E\cos\omega t, 0)$. Within the continuous energy spectrum [Eq. (2)], the electron dynamics can be described by the energy conservation law, $e\mathbf{v}\mathbf{E} = \partial\varepsilon_e(\mathbf{k})/\partial t$, where the left part is the energy received by a dressed electron from the driving field per unit time. It follows from the exact solution of the electron-photon Schrödinger problem [8] that the averaged velocity of the dressed electron in the state with the wave vector $\mathbf{k}$ is given by the expression $\mathbf{v}(\mathbf{k}) = (1/\hbar)\partial\varepsilon_e(\mathbf{k})/\partial\mathbf{k}$, which coincides formally with the well-known classical Hamilton equation, $\mathbf{v}(\mathbf{p}) = \partial\varepsilon(\mathbf{p})/\partial\mathbf{p}$, describing the velocity of a particle with an energy $\varepsilon(\mathbf{p})$ and the generalized momentum $\mathbf{p} = \hbar\mathbf{k}$. Substituting this electron velocity, $\mathbf{v}(\mathbf{k})$, into the energy conservation law, we arrive at the conventional dynamics equation:

$$\hbar\frac{d\mathbf{k}}{dt}\bigg|_{|\mathbf{k}|<k_0} = e\mathbf{E}. \tag{3}$$

Since the driving field is substantially weaker than the dressing field, a dressed electron cannot surmount the dynamic Stark gap, $\Delta\varepsilon$, at the border wave vector, $|\mathbf{k}| = k_0$ [see Fig. 1(b)]. Taking this energy barrier into account, one has to complement the semiclassical dynamics equation (3) with the boundary condition:

$$\hbar\frac{d\mathbf{k}}{dt}\bigg|_{|\mathbf{k}|=k_0} = \begin{cases} 0, & e\mathbf{k}\mathbf{E} > 0 \\ e\mathbf{E}, & e\mathbf{k}\mathbf{E} \leqslant 0 \end{cases}. \tag{4}$$

Equations (2)–(4) give the complete description of the single-electron dynamics in the irradiated QW. For definiteness, let us apply them to consider an electron which is initially in the ground state, $\mathbf{k} = 0$ [see the red dot in Fig. 1(b)]. In this case, the electron wave vector depends on time, t, as a function $\mathbf{k}(t) = (k_x(t), 0)$, where

$$k_x(t) = \begin{cases} k_E\sin\omega t, & |k_E\sin\omega t| < k_0 \\ k_0, & k_E\sin\omega t \geqslant k_0 \\ -k_0, & k_E\sin\omega t \leqslant -k_0 \end{cases} \tag{5}$$

and $k_E = eE/\hbar\omega$ is the amplitude of electron oscillations in k space. The oscillating movement of the electron, which arises from the sines in Eq. (5), should result in the emission of electromagnetic waves from the QW. Restricting analysis of the emission by the dipole approximation, we can write the intensity of the emission at the frequency of the nth harmonic, $\omega_n = n\omega$, in the conventional form (see, e.g., Ref. [26]):

$$I_n = \frac{4e^2}{3c^3}|\mathbf{a}_n|^2, \tag{6}$$

where $\mathbf{a}_n$ is the nth coefficient of the Fourier expansion of the electron acceleration, $\mathbf{a} = (a_x, 0)$. It follows from Eq. (2) that the electron acceleration, $a_x = (\dot{v}_x, 0)$, can be written in the dimensionless form as

$$\begin{aligned}\frac{a_x}{a_0} = \frac{\dot{k}_x}{\omega k_0}\Bigg\{&2\left(\frac{m_+}{m_-}\right) + 2\left(\left[\frac{\Delta\varepsilon}{\varepsilon_0}\right]^2 + \left[1 - \frac{k^2}{k_0^2}\right]^2\right)^{-\frac{3}{2}} \\ &\times\left[1 - \frac{k^2}{k_0^2}\right]^2\frac{k_x^2}{k_0^2} + \left(\left[\frac{\Delta\varepsilon}{\varepsilon_0}\right]^2 + \left[1 - \frac{k^2}{k_0^2}\right]^2\right)^{-\frac{1}{2}} \\ &\times\left[1 - \frac{k^2}{k_0^2} - 2\frac{k_x^2}{k_0^2}\right]\Bigg\},\end{aligned} \tag{7}$$

where $a_0 = \hbar k_0 \omega / 2m_+$ is the characteristic electron acceleration. Equations (5)–(7) define the spectrum of electromagnetic emission from the QW, which is discussed below. For definiteness, we will proceed with the analysis of a GaAs-based QW ($\varepsilon_g = 1.39$ eV, $m_e = 0.067\, m_0$, $m_h = 0.47\, m_0$), which is a suitable system for experimental observation of the discussed effects [see the corresponding electron energy spectrum in Fig. 1(d)].

III. RESULTS AND DISCUSSION

The features of the electromagnetic emission from the QW originate from the dynamic Stark gaps, $\Delta\varepsilon$, which take place at the border electron wave vector, $|\mathbf{k}| = k_0$ [see Fig. 1(b)]. Physically, these gaps confine electron oscillations induced by the driving field within the domain $-k_0 \leqslant k_x \leqslant k_0$ and, therefore, crucially affect the emission spectrum. It follows from Eq. (5) that the electron wave vector in Eq. (5) depends on the time, t, as a purely harmonic function, $k_x(t) = k_E \sin \omega t$, if $k_E \leqslant k_0$. As a consequence, the electron acceleration, $\dot{a}_x \sim \dot{k}_x \sim \cos \omega t$, is also a harmonic function in this case. This results in the electromagnetic emission from the QW only with the frequency of the driving field, ω, if $k_E \leqslant k_0$. However, if the amplitude, k_E, satisfies the condition $k_E > k_0$, the electron oscillations [Eq. (5)] are stopped in k space at the border wave vector, k_0. This leads to the "clipped" oscillations of both the wave vector, $k_x(t)$, and the acceleration, $a_x(t)$, which are plotted in Fig. 2(a). The expansion of the clipped oscillations of the acceleration, $a_x(t)$, into the Fourier series leads to nonzero intensities [Eq. (6)] with multiple frequencies, $\omega_n = n\omega$. These intensities are plotted in Fig. 2(b) as I_n/I_0, where $I_0 = (e\hbar\omega k_0/m^+c)^2/3c$ is the characteristic intensity. It should be noted that the Fourier expansion of the acceleration, $a_x(t)$, pictured in Fig. 2(a), has only odd harmonics with $n = 1,3,5,\ldots$. Therefore, corresponding odd harmonics of the intensity, I_n, appear in the emission spectrum plotted in Fig. 2(b). As expected, only the harmonic with $n = 1$ is significant in Fig. 2(b) for low driving field amplitudes, $E/E_0 \ll 1$, where $E_0 = \hbar\omega k_0/e$ is the characteristic field strength. As we keep on increasing the driving field amplitude, E, other harmonics of the emission with $n > 1$ come into play in Fig. 2(b). As a consequence, a frequency comb of the electromagnetic emission from the QW appears.

It follows from the above that the discussed mechanism of high-frequency generation arises from the nonparabolic area of the electron energy spectrum [Eq. (2)], which takes place near the border electron wave vector, k_0. A physically similar mechanism exists also in semiconductor QWs with strongly nonparabolic electron dispersion [27,28] and superlattices [29]. However, in these systems the nonparabolic region lies very far from the band edge. Therefore, the driving field should be very strong for high-frequency generation. In contrast to this case, the present effect arises from the dynamic Stark gaps which can be induced by a dressing field very close to the band edge (i.e., the border wave vector, k_0, can be very small). As a consequence, the generation appears for a relatively weak driving field. The high-frequency generation in such a near-band-edge regime (which, particularly, corresponds to low electron densities) is the main advantage of the present mechanism. It should be noted that the minimal value of

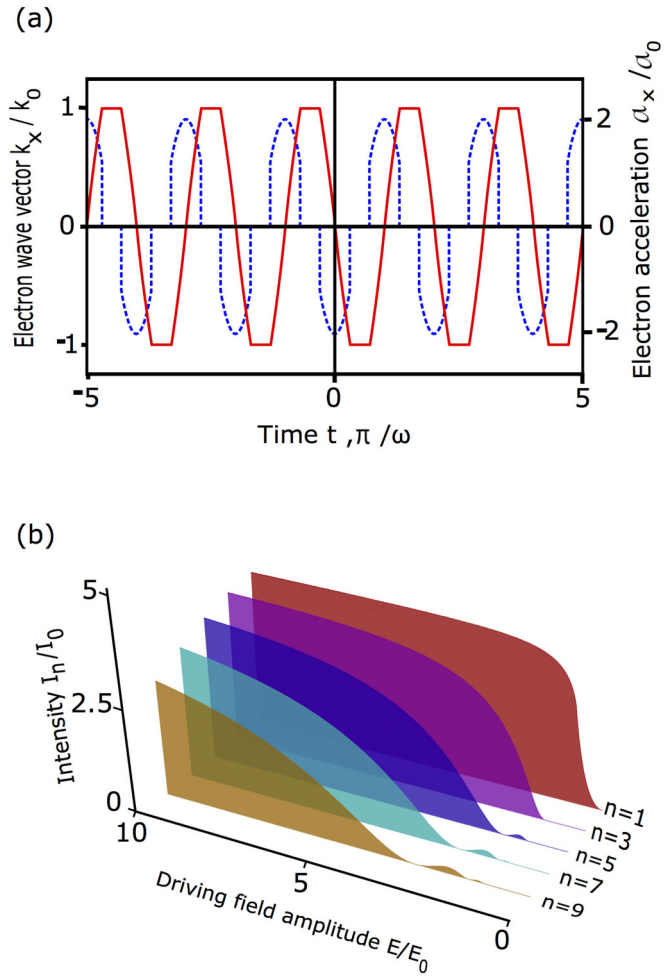

FIG. 2. Scheme of the single-electron electromagnetic emission from the quantum well with the Stark gap $\Delta\varepsilon/\varepsilon_0 = 50$. (a) Oscillation dynamics of the electron wave vector, k_x/k_0 (the blue dashed line), and electron acceleration, a_x/a_0 (the red solid line), for the driving field amplitude $E/E_0 = 1.14$. (b) Intensity of the electromagnetic emission, I_n, with the different frequencies, $\omega_n = n\omega$, as a function of the driving field amplitude, E.

the border electron wave vector, k_0, is restricted only by the Heisenberg uncertainty relation. Namely, the condition $k_0 l \gg 1$ should be satisfied, where l is the mean free path of electrons in the QW. Since the path, l, is macroscopically large in state-of-the-art QWs, the border wave vector, k_0, can be very small.

To go from the considered single-electron model to the case of a 2DEG in real semiconductor QWs (see, e.g., Ref. [30]), we have to make several assumptions. To neglect excitonic effects and inter-sub-band electron dynamics, let us assume that the field frequencies are far from both the excitonic frequency and the frequencies corresponding to inter-sub-band electron transitions. To avoid the destructive effect of scattering processes on the electron oscillations, we will assume that the driving field frequency, ω, is high enough to meet the condition $\omega\tau \gg 1$, where τ is the mean free time of conduction electrons restricted by the electron scattering with phonons and impurities. In modern QWs, this condition can be easily satisfied for driving field frequencies, ω, starting from the

subterahertz range. It should be noted that the simple model that only accounts for intraband acceleration and ignores all scattering is already sufficient to successfully describe the high-harmonic generation in various nonlinear systems (see, e.g., Refs. [31,32]). Particularly, more advanced studies (e.g., based on the Bloch equations technique [33,34]) do not dramatically change the results from the simple model. It should be noted also that the confinement potential of the QW does not influence the discussed effect since the polarization vector of the field lies in the plane of the QW [see Fig. 1(a)]. As to temperature, it should be less than the Stark gap to avoid the thermal excitation of electrons over the gap. In typical semiconductor materials, the gap is of meV scale for the dressing field amplitudes $\widetilde{E} \sim 10^7$ V/m [23].

To extend the single-electron model to the case of a multielectron system in the QW, let us consider a degenerate 2DEG with the Fermi wave vector $k_F < k_0$, which fills electron states [Eq. (2)] at zero temperature. Physically, the electromagnetic emission from the 2DEG can be described within the same model [Eqs. (1)–(7)], but complemented with the Pauli principle. The difference between the single-electron and the multielectron models is illustrated schematically in Fig. 3(a). Namely, the distribution of the 2DEG in the k space can be described by the Fermi circle [see the red line in Fig. 3(a)]. Under the driving field, E, all electrons oscillate along the x axis with different amplitudes [see the green arrows in Fig. 3(a)], which are restricted by the Pauli principle and strongly depend on initial positions of the electrons in k space [see the violet dots in Fig. 3(a)]. As a result, in contrast to the single-electron model, not all electrons can reach the gap at the border wave vector k_0 [see the blue circle in Fig. 3(a)]. Taking the Pauli principle into account, Eq. (5) for an electron from the 2DEG should be rewritten as

$$k_x(t) = \begin{cases} k_x(0) + k_E \sin\omega t, & k_x^- < k_E \sin\omega t < k_x^+ \\ k_x(0) + k_x^+, & k_E \sin\omega t \geqslant k_x^+ \\ k_x(0) + k_x^-, & k_E \sin\omega t \leqslant k_x^- \end{cases}, \quad (8)$$

where $k_x^{\pm} = \pm(\sqrt{k_0^2 - k_y^2} - \sqrt{k_F^2 - k_y^2})$ and $k_x^2(0) + k_y^2 \leqslant k_F^2$. Substituting Eq. (8) into Eq. (7) and performing summation of the electron acceleration [Eq. (7)] over filled electron states, we arrive at the total acceleration of the multielectron system, **a**. Assuming the QW size to be less than the wavelength of the electromagnetic emission, the emission intensity at the frequency $\omega_n = n\omega$ can be described by Eq. (6). As a result, we arrive at the intensities of different harmonics, I_n, which are plotted in Figs. 3(b) and 3(c). Due to the contribution from many electrons, the radiation emitted from the 2DEG is much stronger than the radiation emitted by a single electron [see Figs. 2(b) and 3(b)]. It should be noted that the Fermi energy in GaAs-based QWs can be easily controlled by the gate voltage without doping. If we increase the Fermi wave vector, k_F, the intensities, I_n, also increase since the total number of electrons increases [see Fig. 3(c)]. However, the intensities, I_n, start to decrease if the Fermi wave vector, k_F, comes very close to k_0 [see Fig. 3(c)]. Indeed, in this case a large number of electrons have insufficient empty states in which to oscillate. It should be noted also that the Fermi energies in Figs. 3(b) and 3(c) lie in the sub-meV range. This corresponds to very low electron densities, such that electron-electron processes

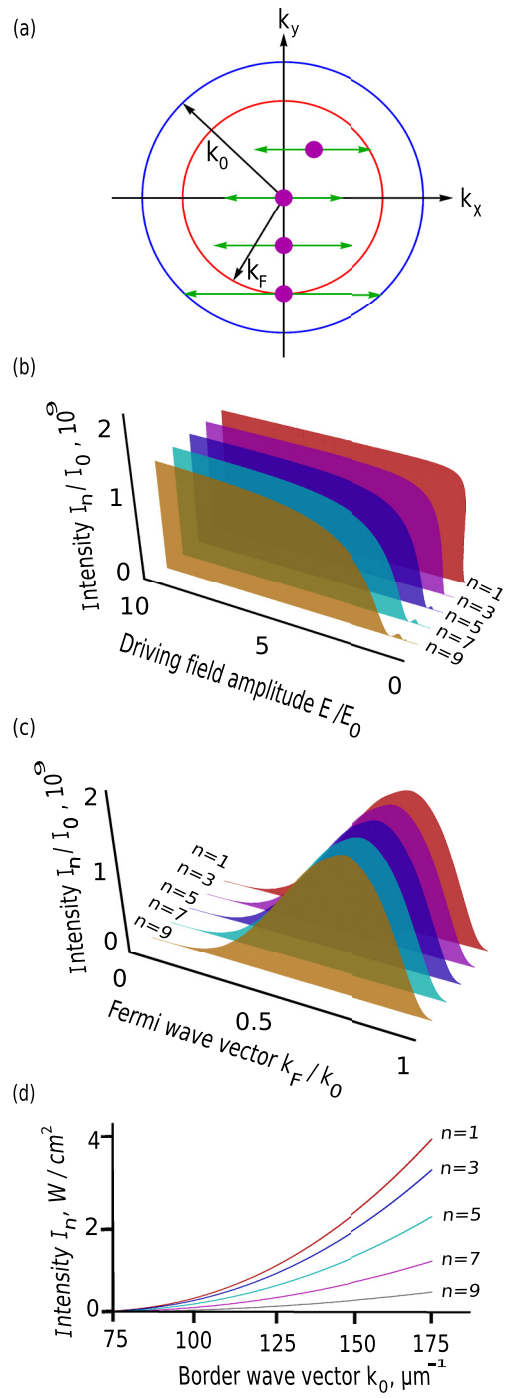

FIG. 3. Scheme of the multielectron electromagnetic emission from the quantum well. (a) Sketch of electron oscillations under the driving field. (b) Intensity of the electromagnetic emission, I_n, with the different frequencies $\omega_n = n\omega$, as a function of the driving field amplitude E for the Stark gap $\Delta\varepsilon/\varepsilon_0 = 50$ and the Fermi wave vector $k_F/k_0 = 0.7$. (c) Intensity of the electromagnetic emission, I_n, as a function of the Fermi wave vector, k_F, for the the Stark gap $\Delta\varepsilon/\varepsilon_0 = 50$ and the driving field amplitude $E/E_0 = 9.8$. (d) Intensity of the electromagnetic emission, I_n, from a GaAs-based QW with the planar dimensions $100 \times 100\,\mu$m as a function of the border wave vector, k_0, for the the Stark gap $\Delta\varepsilon = 5$ meV, the characteristic wave-vector difference, $k_0 - k_F = 25\ \mu\text{m}^{-1}$, and the driving field with the frequency $\omega = 10^{12}$ rad/s and the irradiation intensity $I = 1\,\text{kW/cm}^2$.

do not affect our results and can be neglected. Particularly, the characteristic energy of electron-electron interaction is also of sub-meV scale and, therefore, sufficiently less than the Stark gap induced by the dressing field. The emission power associated with each harmonic, I_n, as a function of the border wave vector, k_0, is plotted in Fig. 3(d). Tuning the photon energy of the dressing field, $\hbar\omega_0$, we can easily control the border wave vector, k_0. If the difference of the characteristic wave vectors, $\Delta k = k_0 - k_F$, is fixed, the increasing of the border wave vector, k_0, results in increasing the total number of electrons. This leads to an enhancement of the output power [see Fig. 3(d)]. But when the border wave vector, k_0, becomes too large, many electrons cannot reach the Stark gaps. As a result, only the first few harmonics gain power and the power of higher harmonics starts to decrease.

The discussed mechanism of electromagnetic emission from the QW looks most attractive for the generation of frequency combs in the terahertz range. Indeed, applying a driving field with the subterahertz frequency, $\omega = 10^{12}$ rad/s, we can effectively produce the terahertz emission with the frequencies $\omega_n = n\omega$ ($n = 3,5,7,\ldots$) and the intensities of a few W/cm^2 [see Fig. 3(d)]. It should be noted that frequency combs are highly sought for making optical clocks, for measuring fundamental constants accurately [35], for high-resolution molecular spectroscopy [36], etc. Traditionally, frequency combs are generated using pulsed lasers [37] and quantum cascade lasers [38,39]. In contrast to these systems, the present comb emitter is very compact. This is important since the search for compact reliable sources of terahertz emission is one of the exciting fields of modern applied physics. In particular, terahertz scattering processes between polariton branches [40–42], inter-sub-band polaritons [43], dipolaritons [44], and different orbital states [45,46] have been considered. Transitions between direct and indirect exciton states, where nonlinearity allows continuous oscillation and terahertz output as a result of parametric instability, have also been studied [47,48]. Moreover, bosonic cascade lasers in which multiple terahertz transitions can be chained have been proposed [49–51]. It should be noted that terahertz frequency combs from exciton-polariton systems have also been proposed, but their expected efficiency is largely unknown [52]. It follows from the above that the present theory describing the efficient terahertz emission from the strongly coupled electron-light system in a QW fits well current tendencies in terahertz physics.

In conclusion, we have demonstrated theoretically that a semiconductor QW irradiated by a two-mode electromagnetic field can serve as an effective source of a terahertz frequency comb. Physically, the discussed nonlinear optical effect arises from the dynamic Stark gaps in the electron energy spectrum of a QW, which strongly modify the electron dynamics in the QW and result in the terahertz emission. Since the parameters affecting the terahertz emission from the QW can be tuned by irradiation, the present theory paves a way to optically controlled QW-based terahertz emitters.

ACKNOWLEDGMENTS

This paper was partially supported by the Ministry of Education of Singapore AcRF Tier 2 (Project No. MOE2015-T2-1-055), Russian Foundation for Basic Research (Project No. 17-02-00053), and Ministry of Education and Science of Russian Federation (Project No. 3.4573.2017/6.7).

[1] M. O. Scully and M. S. Zubairy, *Quantum Optics* (Cambridge University, Cambridge, England, 2001).

[2] C. Cohen-Tannoudji, J. Dupont-Roc, and G. Grynberg, *Atom-Photon Interactions: Basic Processes and Applications* (Wiley, Weinheim, 2004).

[3] P. Hänggi, Driven quantum systems, in *Quantum Transport and Dissipation*, edited by T. Dittrich, P. Hänggi, G.-L. Ingold, B. Kramer, G. Schön, and W. Zwerger (Wiley, Weinheim, 1998).

[4] S. Kohler, J. Lehmann, and P. Hänggi, Driven quantum transport on the nanoscale, Phys. Rep. **406**, 379 (2005).

[5] M. Bukov, L. D'Alessio, and A. Polkovnikov, Universal high-frequency behavior of periodically driven systems: From dynamical stabilization to Floquet engineering, Adv. Phys. **64**, 139 (2015).

[6] M. Holthaus, Floquet engineering with quasienergy bands of periodically driven optical lattices, J. Phys. B **49**, 013001 (2016).

[7] M. Wagner, H. Schneider, D. Stehr, S. Winner, A. M. Andrews, S. Schartner, G. Strasser, and M. Helm, Observation of the Intraexciton Autler-Townes Effect in GaAs/AlGaAs Semiconductor Quantum Wells, Phys. Rev. Lett. **105**, 167401 (2010).

[8] O. V. Kibis, Persistent current induced by quantum light, Phys. Rev. B **86**, 155108 (2012).

[9] M. Teich, M. Wagner, H. Schneider, and M. Helm, Semiconductor quantum well excitons in strong, narrowband terahertz fields, New J. Phys. **15**, 065007 (2013).

[10] S. Morina, O. V. Kibis, A. A. Pervishko, and I. A. Shelykh, Transport properties of a two-dimensional electron gas dressed by light, Phys. Rev. B **91**, 155312 (2015).

[11] K. Dini, O. V. Kibis, and I. A. Shelykh, Magnetic properties of a two-dimensional electron gas strongly coupled to light, Phys. Rev. B **93**, 235411 (2016).

[12] I. G. Savenko, O. V. Kibis, and I. A. Shelykh, Asymmetric quantum dot in a microcavity as a nonlinear optical element, Phys. Rev. A **85**, 053818 (2012).

[13] G. Yu. Kryuchkyan, V. Shahnazaryan, O. V. Kibis, and I. A. Shelykh, Resonance fluorescence from an asymmetric quantum dot dressed by a bichromatic electromagnetic field, Phys. Rev. A **95**, 013834 (2017).

[14] O. V. Kibis, Dissipationless Electron Transport in Photon-Dressed Nanostructures, Phys. Rev. Lett. **107**, 106802 (2011).

[15] H. Sigurdsson, O. V. Kibis, and I. A. Shelykh, Optically induced Aharonov-Bohm effect in mesoscopic rings, Phys. Rev. B **90**, 235413 (2014).

[16] F. K. Joibari, Ya. M. Blanter, and G. E. W. Bauer, Light-induced spin polarizations in quantum rings, Phys. Rev. B **90**, 155301 (2014).

[17] K. L. Koshelev, V. Yu. Kachorovskii, and M. Titov, Resonant inverse Faraday effect in nanorings, Phys. Rev. B **92**, 235426 (2015).

[18] T. Oka and H. Aoki, Photovoltaic Hall effect in graphene, Phys. Rev. B **79**, 081406 (2009).

[19] S. V. Syzranov, Ya. I. Rodionov, K. I. Kugel, and F. Nori, Strongly anisotropic Dirac quasiparticles in irradiated graphene, Phys. Rev. B **88**, 241112 (2013).

[20] P. M. Perez-Piskunow, G. Usaj, C. A. Balseiro, and L. E. F. Foa Torres, Floquet chiral edge states in graphene, Phys. Rev. B **89**, 121401(R) (2014).

[21] M. M. Glazov and S. D. Ganichev, High frequency electric field induced nonlinear effects in graphene, Phys. Rep. **535**, 101 (2014).

[22] O. V. Kibis, K. Dini, I. V. Iorsh, and I. A. Shelykh, All-optical band engineering of gapped Dirac materials, Phys. Rev. B **95**, 125401 (2017).

[23] S. P. Goreslavskii and V. F. Elesin, Electronic properties of a semiconductor in the field of a strong electromagnetic field, JETP Lett. **10**, 316 (1969).

[24] Q. T. Vu, H. Haug, O. D. Mücke, T. Tritschler, M. Wegener, G. Khitrova, and H. M. Gibbs, Light-Induced Gaps in Semiconductor Band-To-Band Transitions, Phys. Rev. Lett. **92**, 217403 (2004).

[25] Y. H. Wang, H. Steinberg, P. Jarillo-Herrero, and N. Gedik, Observation of Floquet-Bloch states on the surface of a topological insulator, Science **342**, 453 (2013).

[26] L. D. Landau and E. M. Lifshitz, *The Classical Theory of Fields* (Pergamon, Oxford, 1971).

[27] P. Haljan, T. Fortier, P. Hawrilyak, P. B. Corkum, and M. Yu. Ivanov, High harmonic generation and level bifurcation in strongly driven quantum wells, Laser Phys. **13**, 452 (2003).

[28] J. Hurst, K. Leveque-Simon, P.-A. Hervieux, and G. Manfredi, High-harmonic generation in a quantum electron gas trapped in a nonparabolic and anisotropic well, Phys. Rev. B **93**, 205402 (2016).

[29] T. Hyart, N. V. Alexeeva, J. Mattas, and K. N. Alekseev, Terahertz Bloch Oscillator with a Modulated Bias, Phys. Rev. Lett. **102**, 140405 (2009).

[30] H. Haug and S. W. Koch, *Quantum Theory of the Optical and Electronic Properties of Semiconductors* (World Scientific, Singapore, 1998).

[31] O. D. Mücke, Isolated high-order harmonics pulse from two-color-driven Bloch oscillations in bulk semiconductors, Phys. Rev. B **84**, 081202(R) (2011).

[32] T. T. Luu, M. Garg, S. Yu. Kruchinin, A. Moulet, M. Th. Hassan, and E. Goulielmakis, Extreme ultraviolet high-harmonic spectroscopy of solids, Nature (London) **521**, 498 (2015).

[33] D. Golde, T. Meier, and S. W. Koch, High harmonics generated in semiconductor nanostructures by the coupled dynamics of optical inter- and intraband excitations, Phys. Rev. B **77**, 075330 (2008).

[34] O. Schubert, M. Hohenleutner, F. Langer, B. Urbanek, C. Lange, U. Huttner, D. Golde, T. Meier, M. Kira, S. W. Koch, and R. Huber, Sub-cycle control of terahertz high-harmonic generation by dynamical Bloch oscillations, Nat. Photonics **8**, 119 (2014).

[35] T. Rosenband, D. B. Hume, P. O. Schmidt, C. W. Chou, A. Brusch, L. Lorini, W. H. Oskay, R. E. Drullinger, T. M. Fortier, J. E. Stalnaker, S. A. Diddams, W. C. Swann, N. R. Newbury, W. M. Itano, D. J. Wineland, and J. C. Bergquist, Frequency ratio of Al+ and Hg+ single-ion optical clocks; Metrology at the 17th decimal place, Science **319**, 1808 (2008).

[36] A. Florian, M. J. Thorpe, K. C. Cossel, and J. Ye, Cavity-enhanced direct frequency comb spectroscopy: Technology and applications, Annu. Rev. Anal. Chem. **3**, 175 (2010).

[37] B. Ferguson and X. C. Zhang, Materials for terahertz science and technology, Nat. Mater. **1**, 26 (2002).

[38] D. Burghoff, T. Y. Kao, N. Han, C. W. I. Chan, X. Cai, Y. Yang, D. J. Hayton, J. R. Gao, J. L. Reno, and Q. Hu, Terahertz laser frequency combs, Nat. Photonics **8**, 462 (2014).

[39] S. Bartalini, L. Consolino, P. Cancio, P. De Natale, P. Bartolini, A. Taschin, M. De Pas, H. Beere, D. Ritchie, M. S. Vitiello, and R. Torre, Frequency-Comb-Assisted Terahertz Quantum Cascade Laser Spectroscopy, Phys. Rev. X **4**, 021006 (2014).

[40] K. V. Kavokin, M. A. Kaliteevski, R. A. Abram, A. V. Kavokin, S. Sharkova, and I. A. Shelykh, Stimulated emission of terahertz radiation by exciton-polariton lasers, Appl. Phys. Lett. **97**, 201111 (2010).

[41] I. G. Savenko, I. A. Shelykh, and M. A. Kaliteevski, Nonlinear Terahertz Emission in Semiconductor Microcavities, Phys. Rev. Lett. **107**, 027401 (2011).

[42] S. Huppert, O. Lafont, E. Baudin, J. Tignon, and R. Ferreira, Terahertz emission from multiple-microcavity exciton-polariton lasers, Phys. Rev. B **90**, 241302(R) (2014).

[43] S. De Liberato, C. Ciuti, and C. C. Phillips, Terahertz lasing from intersubband polariton-polariton scattering in asymmetric quantum wells, Phys. Rev. B **87**, 241304 (2013).

[44] O. Kyriienko, O. V. Kibis, and I. A. Shelykh, Floquet control of dipolaritons in quantum wells, Opt. Lett. **42**, 2398 (2017).

[45] A. V. Kavokin, I. A. Shelykh, T. Taylor, and M. M. Glazov, Vertical Cavity Surface Emitting Terahertz Laser, Phys. Rev. Lett. **108**, 197401 (2012).

[46] A. A. Pervishko, T. C. H. Liew, V. M. Kovalev, I. G. Savenko, and I. A. Shelykh, Nonlinear effects in multi-photon polaritonics, Opt. Express **21**, 15183 (2013).

[47] O. Kyriienko, A. V. Kavokin, and I. A. Shelykh, Superradiant Terahertz Emission by Dipolaritons, Phys. Rev. Lett. **111**, 176401 (2013).

[48] K. Kristinsson, O. Kyriienko, T. C. H. Liew, and I. A. Shelykh, Continuous terahertz emission from dipolaritons, Phys. Rev. B **88**, 245303 (2013).

[49] T. C. H. Liew, M. M. Glazov, K. V. Kavokin, I. A. Shelykh, M. A. Kaliteevski, and A. V. Kavokin, Proposal for a Bosonic Cascade Laser, Phys. Rev. Lett. **110**, 047402 (2013).

[50] T. C. H. Liew, Y. G. Rubo, A. S. Sheremet, S. De Liberato, I. A. Shelykh, F. P. Laussy, and A. V. Kavokin, Quantum statistics of bosonic cascades, New J. Phys. **18**, 023041 (2016).

[51] M. A. Kaliteevski, K. A. Ivanov, G. Pozina, and A. J. Gallant, Single and double bosonic stimulation of THz emission in polaritonic systems, Sci. Rep. **4**, 5444 (2014).

[52] K. Rayanov, B. L. Altshuler, Y. G. Rubo, and S. Flach, Frequency Combs with Weakly Lasing Exciton-Polariton Condensates, Phys. Rev. Lett. **114**, 193901 (2015).